Article

Journal of the Brazilian Chemical Society

https://dx.doi.org/10.21577/0103-5053.20240001

J. Braz. Chem. Soc. **2024**, *35*, 6, e-20240001, 1-14

In silico and *in vitro* Studies Evaluating the Promising Antiureolytic Activity of Schiff's Base 4-(3-Hydroxybenzylideneamino)phenol and Its Amine Derivative

Caroline S. Dohanik,[a] Camila P. Pereira,[b] Breno G. F. de Oliveira,[b] Igor J. S. Nascimento,[c] Amanda Luise A. Nascimento,[c] Josué C. C. Santos,[c] Thiago M. de Aquino,[c] Rachel O. Castilho,[a] Luzia V. Modolo,[d] Ângelo de Fátima*[,b] and Gisele A. C. Goulart*[,a]

[a]*Departamento de Produtos Farmacêuticos, Faculdade de Farmácia, Universidade Federal de Minas Gerais, 31270-901 Belo Horizonte-MG, Brazil*

[b]*Departamento de Química, Universidade Federal de Minas Gerais, 31270-901 Belo Horizonte-MG, Brazil*

[c]*Instituto de Química e Biotecnologia, Universidade Federal de Alagoas, 57072-900 Maceió-AL, Brazil*

[d]*Departamento de Botânica, Universidade Federal de Minas Gerais, 31270-901 Belo Horizonte-MG, Brazil*

Urea is the most widely used nitrogen fertilizer worldwide. However, ammonia volatilization, resulting from applying urea to the soil surface, causes economic and environmental losses; thus, urease inhibitors have been developed to mitigate these losses. In this work, the anti-ureolytic activity of Schiff's base 4-(3-hydroxybenzylideneamino) phenol (**3B4**) and its amine-derived (**3B4a**) was evaluated. The most promising urease inhibitor in soil was **3B4** (55.0 ± 3.9% inhibition), with comparable results to *N*-(butyl) thiophosphoric triamide ($p = 0.659$). In the *in vitro* analysis (*Canavalia ensiformis*), the results of anti-ureolytic activity were similar, 22.6 ± 6.9% for **3B4** and 24.2 ± 9.6% for 3B4a. Biophysical interaction studies were also carried out through molecular docking studies and molecular fluorescence spectroscopy. These studies showed that both substances are preferentially competitive inhibitors, with the interaction between **3B4a** and urease forming a more stable complex. In the analysis by Fourier transform infrared spectroscopy, no interaction was observed when **3B4** or **3B4a** was mixed with urea (1:1) for 48 h, providing evidence of compatibility. Thus, the Schiff base **3B4** and its corresponding amine **3B4a** may represent potential additives for urea fertilization aiming to assist in the urease inhibition process.

Keywords: urease, urea, urease inhibitors, Schiff bases, amine derivative, competitive inhibitors

Introduction

Nitrogen (N) is essential to produce macromolecules and small key molecules by plants, such as chlorophyll. Although it is abundant in the atmosphere, representing about 80% of its volume, N is biologically unavailable due to its highly stable gas form.[1,2] But, through the Haber-Bosch process, it is possible to obtain N fertilizers, contributing to high productivity in current crops,[1,2] as 30 to 50% of the agricultural production is attributed to introducing mineral fertilizers, including synthetic N. Thus, feeding about 48% of the world's population is due to using N fertilizers,[1,3] highlighting the importance of this element in agriculture to maintain the food supply. Urea is the most widely used synthetic nitrogen fertilizer, accounting for more than 70% of fertilizer use worldwide.[4] The preference for urea is justified by its high N content for molecule (46.6% in mass), chemical stability, low production costs and ease of mixing with other fertilizers.[5-7] However, urea can undergo hydrolysis when applied to the soil, and this process is associated with the urease enzyme.[8,9]

The urease enzymes occur widely in nature, as in soils, playing a decisive role in N metabolism.[6] This enzyme was crystallized for the first time by James B. Sumner, who received, in 1946, the Nobel Prize in Chemistry for

*e-mail: adefatima@qui.ufmg.br; gacg@ufmg.br
Editor handled this article: Brenno A. D. Neto

showing that enzymes can be isolated in crystal form.[10,11] Ureases were the first example of a nickel metalloenzyme cited in the literature.[6,12] This enzyme catalyzes the hydrolysis of urea in ammonia and carbamate, which spontaneously decomposes into carbonic acid and more ammonia.[13,14] Inorganic nitrogen pollution from ammonia emissions can contribute to the acidification of aquatic and terrestrial ecosystems, eutrophication, and reduction of biodiversity.[15-19] The use of urea can also contribute directly (nitrification and denitrification) and indirectly (NH_3 volatilization) to N_2O emissions.[20,21] This gas contributes to the greenhouse effect and destruction of stratospheric ozone.[1,9] In addition, higher ammonia emissions can favor aerosol formations, decreasing visibility,[22] and favoring the formation of particles smaller than 2.5 μm in diameter ($PM_{2.5}$),[23] which negatively impacts human health.[24]

The degradation of urea by urease also generates economic losses for farmers since fewer nutrients are available to plants, affecting productivity.[5] Pinto *et al.*[25] estimated that approximately 5.26% of the resource invested in applying 400 kg urea *per* ha *per* year in an area of 100 ha was lost due to ammonia volatilization and denitrification. Thus, the development of alternatives to improve the efficiency of N fertilizers is desirable from both an environmental and an economic point of view.[26]

One of the strategies to improve urea performance and reduce environmental impacts is the use of urease inhibitors.[7,21,27-29] The *N*-(butyl) thiophosphoric triamide (NBPT) is the most commercially used urease inhibitor in agriculture, being able to delay urea hydrolysis and decrease ammonia volatilization.[5,21,29,30] However, studies have shown that the stability of NBPT is a concern since its degradation occurs over time when applied to urea and is dependent on temperature and pH.[5,8,31,32] Thus, it is necessary to increase the supply of urease inhibitors that are effective in different types of soils, compatible with urea, efficient in low concentrations, and safe for the environment and human health.[26]

Among the new substances synthesized by our research group, Schiff bases have stood out for their ease of synthesis, low cost, and higher thermal stability than NBPT, as reported in a patent document.[33] Among 71 synthesized substances, eight stood out (Figure 1), and substance 3-hydroxybenzaldehyde (Scheme 1, **3B4**) was chosen because it presented promising results in urease inhibition experiments *in vitro* and soil, in addition to not harming germination and plant development.[33,34]

In this work, an amine analog, 4-(3-hydroxybenzylidene-amino) phenol (Scheme 1, **3B4a**), derived from Schiff base **3B4**, was compared regarding its anti-ureolytic activity in soil and *in vitro*. Molecular docking and molecular fluorescence spectroscopy studies were performed to understand better the structural features responsible for the anti-ureolytic activity and the interaction of the assets with the urease active site. Finally, the interaction of **3B4** and **3B4a** with urea was also evaluated, aiming at the application of these substances as additives to increase the efficiency of fertilizers.

Experimental

Chemicals

All chemicals were obtained from commercial suppliers and used without further purification. Urease (from jack

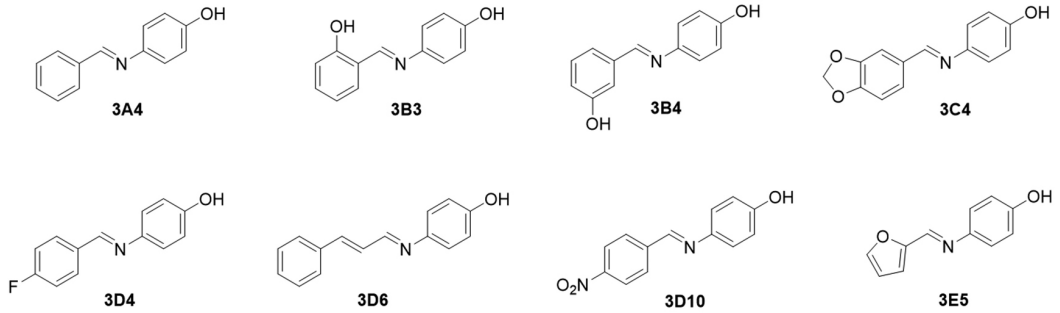

Figure 1. Schiff bases with high anti-ureolytic activity synthesized by our research groups.[33,34]

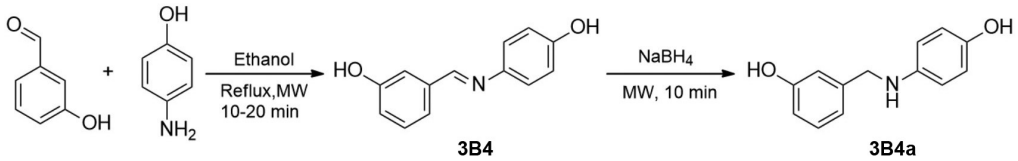

Scheme 1. Synthesis of substances **3B4** and **3B4a** under microwave irradiation (MW). Reaction conditions and reagents: **3B4**: 3-hydroxybenzaldehyde (1 mol), 4-hydroxyaniline (1 mol), solubilized in ethanol and irradiated in microwave reactor during 10-20 min (72%). **3B4a**: 4-(3-hydroxybenzylideneamino) phenol (1 mol), $NaBH_4$ (2 mol), solubilized in ethanol followed by addition of $NaBH_4$, and irradiated in microwave reactor during 10 min (76%).

beans, nominal activity 40.1 units mg^{-1} solid) was obtained from Sigma-Aldrich (St. Louis, USA). Uncorrected melting points were determined in a melting point meter PF 1500 FARMA (Gehaka, São Paulo, Brazil). Reactions under microwave irradiation (MW) were carried out in a CEM-Microwave-Enhanced Life reactor (Matthews, USA). The ^{1}H nuclear magnetic resonance (NMR) and ^{13}C NMR spectra were recorded on a Bruker Avance DRX/400 (Bruker, Billerica, USA). Chemical shift values (δ) were given in parts *per* million (ppm). Fourier transform infrared spectroscopy (FTIR) spectra were recorded in a Spectrometer One PerkinElmer (PerkinElmer, Waltham, USA).

A microplate spectrophotometer (Multiskan FC, Thermo Scientific, Waltham, USA), a centrifuged model Heraeus Fresco 17 Centrifuge (Thermo Scientific, Waltham, USA), and a Shaker MaxQ4000 (Thermo Scientific, Waltham, USA) were used to study the enzymatic activity of urease inhibition.

Synthesis of **3B4** and **3B4a**

Synthesis of **3B4** (Scheme 1) was performed using the 3-hydroxybenzaldehyde (10 mmol) (Sigma-Aldrich, St. Louis, USA) and 4-hydroxyaniline (10 mmol) (Sigma-Aldrich, St. Louis, USA) in ethanol. The mixture was placed in a microwave reactor and irradiated at reflux temperature, with a ramp time of 4 min and reaction time of 10 to 20 min under maximum agitation. Purification was performed by recrystallization using hexane:ethyl acetate (1:1). The product was characterized by melting point analysis, NMR (^{1}H and ^{13}C), and FTIR spectroscopy.

The **3B4** amine derivative (Scheme 1), compound **3B4a**, was prepared according to Byung and Sang,[35] with modifications. Briefly, 5 mmol of **3B4** were solubilized in ethanol, followed by a slow addition of sodium borohydride ($NaBH_4$; in a 1:2 ratio). The mixture was placed under a microwave irradiation reactor for 10 min and then subjected to extraction with ethyl acetate and distilled water. The organic phase was collected, dried with sodium sulfate (Na_2SO_4), and evaporated after filtration. The product was characterized by melting point analysis, NMR (^{1}H and ^{13}C), and IR spectroscopy.

4-(3-Hydroxybenzylideneamino)phenol (**3B4**)

Yield (72%), 7.2 mmol, 1.53 g; mp 192.1-194.3 °C (lit.:[36] 189.0 °C); IR (KBr) ν / cm^{-1} 3306, 1624, 1588, 1506, 1460, 1290, 1270, 1258, 1218, 806, 686; ^{1}H NMR (400 MHz, DMSO-d_6) δ 6.80 (d, 2H, *J* 4.3 Hz), 6.87-6.90 (m, 1H), 7.18 (d, 2H, *J* 4.3 Hz), 7.28-7.30 (m, 2H), 7.33 (s, 1H), 8.51 (s, 1H), 9.50 (s, 1H), 9.64 (s, 1H); ^{13}C NMR (100 MHz, DMSO-d_6) 113.9, 115.7, 118.2, 119.9, 122.5, 129.8, 137.9, 142.6, 156.3, 157.2, 157.7.

3-(((4-Hydroxyphenyl)amino)methyl)phenol (**3B4a**)

Yield (76%), 3.8 mmol, 0.82 g; mp 136.3-138.5 °C (lit.:[37] 153-156 °C); IR (KBr) ν / cm^{-1} 3308, 3260, 1598, 1518, 1476, 1456, 1268, 1232, 1226, 1046, 840, 766, 690; ^{1}H NMR (400 MHz, DMSO-d_6) δ 4.07 (d, 2H, *J* 5.8 Hz), 5.50 (t, 1H, *J* 11.6), 6.40 (d, 2H, *J* 4.3 Hz), 6.49 (d, 2H, *J* 4.3 Hz), 6.55-6.59 (m, 1H), 6.74 (broad sign, 2H), 7.07 (t, 1H, *J* 15.8), 8.37 (s, 1H), 9.26 (s, 1H); ^{13}C NMR (100 MHz, DMSO-d_6) δ 47.6, 113.4, 113.5, 114.0, 115.6, 117.8, 129.1, 141.6, 142.4, 148.2, 157.3.

Inhibitory activity against urease in soil

The anti-ureolytic activity in soil of **3B4** and **3B4a** was evaluated in a dystrophic clayey Red Latosol collected from an agricultural land located in the Brazilian Cerrado (19°28'01.2"S, 44°10'24.5"W), as described by Kandeler and Gerber,[38] with modifications.[39] The physicochemical characteristics of the soil used were 16.40% sand, 23.64% silt, and 59.96% clay; pH 5.8; 10.4 mg dm^3 $P_{(Mehlich)}$; 240 mg dm^{-3} of K^+; 4.44 $cmol_c$ dm^{-3} of Ca^{2+}; 1.17 $cmol_c$ dm^{-3} of Mg^{2+}; 0.06 $cmol_c$ dm^{-3} of Al^{3+}; 2.99 $cmol_c$ dm^{-3} H^+Al, base sum of 6.22 $cmol_c$ dm^{-3} and organic matter equivalent to 3.60 dag kg^{-1}.

The soil was sieved using 2 mm mesh, and samples of 0.5 g, previously activated with water for 24 h, were placed in 15 mL tubes. To evaluate urease inhibition in soil, 500 µM of the test substances were solubilized in ethanol and 80 mM of urea (Merck, Darmstadt, Germany). Samples were incubated in the Shaker (Thermo Scientific, MaxQ4000, Waltham, USA) at 37 °C for 1 h. Reactions were stopped by adding 5 mL of 1 M potassium chloride (KCl) in 1 M hydrochloric acid (HCl). Each system was incubated for a further 30 min and then centrifuged (Thermo Scientific, Heraeus Fresco 17 Centrifuge, Waltham, USA) for 3 min at 10,000 × g. After centrifugation, 100 µL of a solution containing 3.4% (m/v) sodium salicylate, 2.5% (m/v) sodium citrate, 2.5% (m/v) sodium tartrate, and 0.012% (m/v) sodium nitroprusside (SNP) were added to the 20 µL of the supernatant, which was incubated for 15 min at 25 °C and 600 rpm. Each mixture received 0.1 vol of a solution containing 3.0% (m/v) sodium hydroxide (NaOH) in 1% (v/v) sodium hypochlorite, followed by incubation for 1 h at 25 °C in the dark under 600 rpm. The ammonium formed was quantified (λ_{max} = 660 nm) (Multiskan FC, Thermo Scientific, Waltham, USA) with the aid of a calibration curve using ammonium chloride as a standard. All experiments were performed in triplicate

(n = 3) with five technical replicates for each substance. NBPT was used as a reference for urease inhibition.

In vitro inhibitory activity against urease (*Cavanalia ensiformis*)

In vitro urease inhibition studies were conducted to understand the interactions of synthesized substances (**3B4** and **3B4a**) with urease presented in theoretical molecular analyses. Reactions were performed in 20 mM phosphate buffer (pH 7.0) containing 1.0 mM EDTA (ethylenediamine tetraacetic acid), 12.5 mU urease of *C. ensiformis* enzyme (Sigma-Aldrich, St. Louis, USA), 10 mM urea in the presence or absence of each compound-test at 50 μM (solubilized in ethanol).[39] The reactions were incubated at 25 °C for 10 min and stopped by adding 0.5 vol of 1% m/v phenol in 5 mg L^{-1} SNP and 0.7 vol of 0.5% m/v NaOH in 0.1% v/v sodium hypochlorite. The systems were incubated at 50 °C for more 5 min, followed by quantification of NH_4^+ (λ_{max} = 630 nm) (Multiskan FC, Thermo Scientific, Waltham, USA) with the aid of an analytical curve using ammonium chloride as a standard. Hydroxyurea (HU) (Sigma-Aldrich, St. Louis, USA) was used as the inhibitor reference. The experiments were performed in quadruplicate (n = 4) with four repetitions for each substance. In experiments evaluating anti-ureolytic activity, the online software Chemicalize, developed by ChemAxon,[40] was used to predict the pK_a and logP of substances **3B4** and **3B4a**.

Molecular modeling

The docking study was performed with compounds **3B4** and **3B4a** to predict binding conformation, interactions with essential residues, and coordination with the bi-nickel center in the urease's active site. The lowest energy binding poses for derivatives were chosen as the initial conformations for the molecular dynamics (MD) simulations of the protein-ligand complexes for 100 ns to evaluate the complexes' stabilities. Root-mean-square deviation (RMSD) of ligands and root-mean-square fluctuation (RMSF) of protein were calculated based on the analysis of the MD trajectories. Finally, MM-PBSA calculations were performed using the trajectory files obtained after the MD simulations to determine the protein-ligand complexes' binding energy. All simulations were performed according to our research group's previous procedures.[41]

Interaction between inhibitors-urease by molecular fluorescence spectroscopy

The spectrofluorimetric measurements were performed using the Varian Cary Eclipse spectrofluorimeter (Agilent, Santa Clara, USA) with a thermostat provided by a single cell peltier, with 1 cm optical path quartz cuvettes. Substances **3B4**, **3B4a**, NBPT, HU, and urea were used in interaction studies with the enzyme urease (*C. ensiformis*) (Sigma, St. Louis, USA). The stock solutions of the substances were prepared in ethanol, and the urease solutions alone or containing the inhibitors were prepared in 20 mM phosphate buffer (pH = 7.40) and ultrapure water (Milli-Q® purification system, Merck Millipore, Burlington, USA).

Spectrophotometric measurements were performed on a Hitachi U-2010 UV-Vis spectrophotometer (Hitachi, Tokyo, Japan). Based on the absorbance signal (λ_{max} = 280 nm) and the molar extinction coefficient for urease enzyme (54780 M^{-1} cm^{-1}),[42] the urease concentration in the stock solution was calculated.

The spectrofluorimetric interaction studies were performed using 1.0 μM urease, λ_{ex} = 280 nm, λ_{em} = 290 to 420 nm, and the slit was 5/10 nm ($\lambda_{ex}/\lambda_{em}$). Thermodynamic parameters and intermolecular forces involved in the interaction of enzyme and inhibitors were determined based on spectrofluorimetric titrations. The urease concentration was fixed at 1.0 μM, and increasing inhibitor concentrations (5-80 μM) at 23, 30, and 38 °C. The reference signal was established considering the system without the inhibitors under the same conditions. The quenching mechanism was assessed using the Stern-Volmer equation 1:

$$\frac{F_0}{F} = 1 + K_{SV}[Q] \text{ or } \frac{F_0}{F} = 1 + k_q\tau_0[Q] \quad (1)$$

where F_0 and F are the fluorescence intensities in the absence and presence of the ligand, respectively; [Q] is the concentration of the ligand; K_{SV} is the Stern-Volmer quenching constant; k_q is the maximum rate constant for diffusional quenching bimolecular constant in biopolymer systems (2.0×10^{10} M^{-1} s^{-1}); and τ_0 is the average lifetime (10^{-8} s). To evaluate the degree of interaction between the compounds through the binding constant (K_b) and to determine the stoichiometry of the complex formed between urease and the inhibitors (*n*) were used equation 2:

$$\log\left(\frac{F_0 - F}{F}\right) = \log K_b + n\log[Q] \quad (2)$$

where, F_0 and F are the fluorescence intensities in the absence and presence of the ligand, respectively; [Q] is the concentration of the ligand; *n* is the stoichiometric proportion of the supramolecular complex formed between enzyme and inhibitor (number of sites occupied by the ligand in the urease structure); and K_b is the binding constant (expresses the strength of the interaction between the ligand and the macromolecule). The thermodynamic

parameters involved in binding were also determined. The values of enthalpy (ΔH) and entropy (ΔS) were calculated by linearizing the Van't Hoff equation 3:

$$\ln(K_b) = -\frac{\Delta H}{R} \times \left[\frac{1}{T}\right] + \frac{\Delta S}{R} \quad (3)$$

R is the gas constant (8.3144621 J mol^{-1} K^{-1}); T is the experimental temperature (Kelvin); and K_b is the binding constant at a given temperature. To evaluate the process spontaneity, Gibbs free energy (ΔG) was calculated by equation 4:

$$\Delta G = \Delta H - T\Delta S \quad (4)$$

The 3D fluorescence was used to assess conformational changes in the enzyme structure in the presence of the inhibitors. The spectrofluorimetric measurements were performed under the following conditions: 1.0 μM enzyme urease and **3B4** or **3B4a** at 70 μM. The instrumental conditions were the same as in the previous experiments. The interaction of the substrate (urea), the standard inhibitors (HU and NBPT), and the proposed inhibitors (**3B4** and **3B4a**) with the enzyme was evaluated through a competition assay. Spectrofluorimetric titrations of the enzyme (1 μM) with **3B4** and **3B4a** (5-80 μM) were performed in the presence and absence of inhibitors or substrate (10 μM).

Interaction between **3B4** and **3B4a** with urea

The FTIR technique was used to verify the interaction between the proposed inhibitors (**3B4** and **3B4a**) and urea. FTIR spectra were recorded using Spectrum One PerkinElmer equipment with an attenuated total reflectance (ATR) system (PerkinElmer, Waltham, USA), and absorption was measured in wavenumber (cm^{-1}). The analysis was performed with the mixture (1:1) of urea and **3B4** or **3B4a**, crushed with a pestle in an agate mortar. The samples (protected from light) were prepared and analyzed after 0, 24, and 48 h.

Statistical analysis

The results were presented as means ± standard deviations. The Kolmogorov-Smirnov test assessed normality, while homoscedasticity was by Brown-Forsythe. If the data followed a normal distribution and homoscedastic, parametric statistics were used (one-way analysis of variance (ANOVA) test followed by Tukey post-test). Outlier analysis was performed with a 10% Q ROUT test. The s statistical difference was considered significant when p-values < 0.05. Statistical analyzes were performed using GraphPad Prism version 6.01.[43]

Results and Discussion

Synthesis

The imine was obtained from a condensation reaction between 3-hydroxybenzaldehyde and 4-hydroxyaniline with a high yield (72%) and easy preparation. The respective amine is the product of reductive amination of **3B4**, thus guaranteeing a high yield (76%). Both urease inhibitors were characterized by melting point, FTIR, and ^{1}H and ^{13}C NMR (spectra of both substances can be accessed in the Supplementary Information (SI) section), and the values were consistent with the literature.

Evaluation of urease inhibition in soil and *in vitro*

Among the urease inhibitors tested, **3B4** was as efficient as NBPT and inhibited soil ureases by 55.0% on average (Figure 2a, $p = 0.659$). Notably, the imine **3B4** was roughly twice as much potent as the corresponding amine **3B4a** (Figure 2a, $p = 0.006$). The most potent substance in soil, **3B4**, and the corresponding amine were submitted to *in vitro* test with urease from *C. ensiformis*. The anti-ureolytic activity of the substances **3B4** and **3B4a** at 50 μM (22.6 ± 6.9 and 24.2 ± 9.6%, respectively) were similar to that of the reference inhibitor HU (Figure 2b, $p = 0.988$ and $p = 0.991$, respectively).

The difference observed between the activity of **3B4** and **3B4a**, when comparing the *in vitro* and soil results, suggests that the **3B4a** substance may be protonated at the soil pH, becoming more retained in soil colloids, and less available to act as a urease inhibitor. Colloids are mainly responsible for the chemical activity of the soil and have a net negative charge that attracts and retains particles/substances with a positive charge.[44] Using the online software Chemicalize[40] it was possible to obtain the pK_a values of the substances **3B4** and **3B4a** and, from the pK_a values, calculate the distribution of micro species. As can be seen in Figure 3, at the pH of the soil used in the test (5.8), around 98.7% of the substance **3B4** is in its neutral form (Figure 3a, H_2A), compared to 55.8% of the **3B4a** (Figure 3b, H_2B). Thus, the protonation of **3B4a** (43%, Figure 3b, H_3B^+) favors its retention in the soil, which may justify the lower activity (2 times lower) in relation to the **3B4** imine (Figure 2).

In the *in vitro* assay, the influence of the soil matrix is inexistent, showing only the activity of **3B4a** in contact with the enzyme urease. Thus, molecular modeling

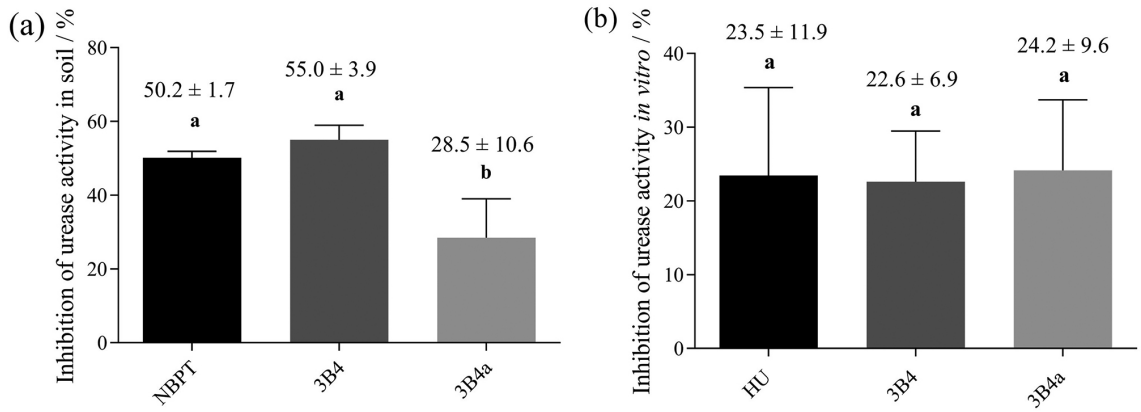

Figure 2. Effect of **3B4** and **3B4a** on soil (a) and *C. ensiformis* (b) ureases. Hydroxyurea (HU) and *N*-(butyl)thiophosphoric triamide (NBPT) were used as reference urease inhibitors. Data were analyzed by one-way ANOVA followed by Tukey post-test at a significance level of 5%. Distinct letters represent statistical differences.

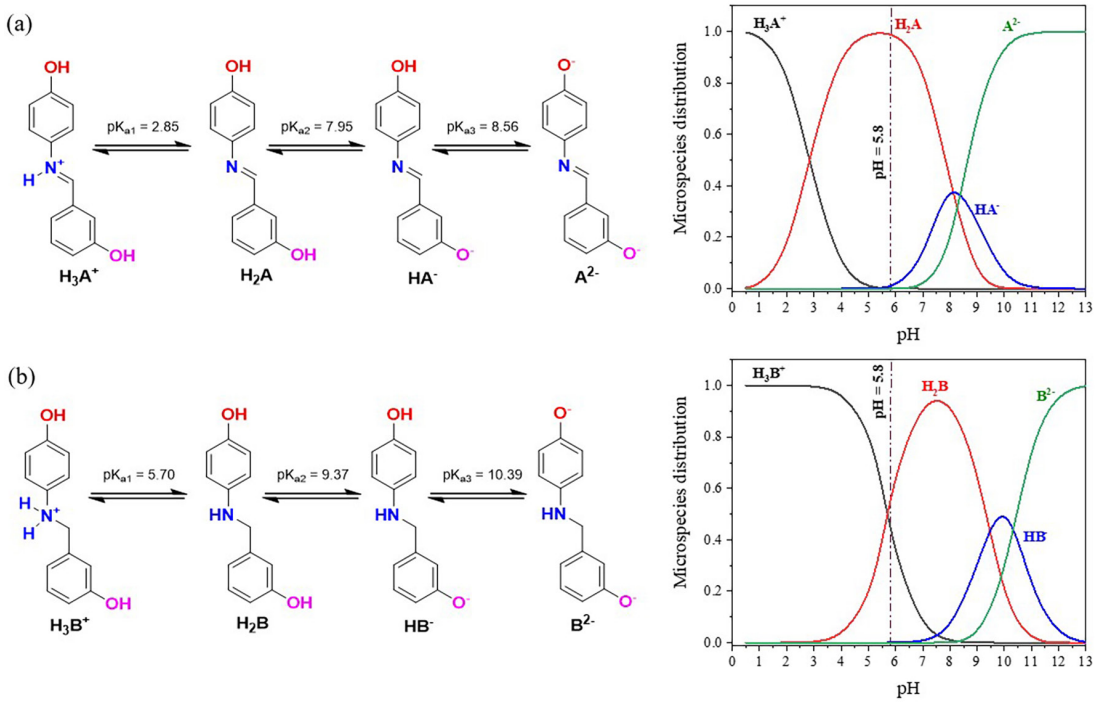

Figure 3. Micro species distribution of **3B4** (a) and **3B4a** (b) at pH 5.8. **3B4** (a) is being considered generically as H_3A^+ (in fully protonated form), while **3B4a** as H_3B^+ (b).

and spectroscopy biophysical studies were proposed to understand which groups are the most important for **3B4** and **3B4a** to act as urease inhibitors and how the interaction between these inhibitors and the enzyme works.

Molecular modeling

The docking simulations revealed that the position of the hydroxyl group in the aromatic ring (3- and 4-position for **3B4** and **3B4a**, respectively) is a critical factor for enzyme inhibition.[45] For amine derivative **3B4a**, the binding conformation showed 4-hydroxyl coordination with the urease's bi-nickel center (Figure 4b). Further stability was due to the formation of some interactions, including conventional hydrogen bonds between the –OH group with carbamylated lysine KCX490 and His409 residues. The analysis of the imine derivative **3B4** revealed traditional hydrogen bonds between the –OH group with His519 and Ala440 residues, and coordination with only one Ni^{II} center, which suggests the formation of a less stable complex, and slightly lower activity. Finally, both compounds performed π-alkyl interactions with Leu589 and π-cation with His585, as well as hydrogen bonds between CME592 and imine or amine groups of **3B4** and **3B4a**, respectively.

These results are in line with the results obtained in *in vitro* tests. When evaluated *in vitro*, the substance

3B4a showed slightly greater antiureolytic activity than **3B4**, since it was completely bioavailable, favoring the formation of a stable complex with urease. It is important to highlight that, although both substances have a hydrophobic profile (solubility studies, Table S1, SI section), in the study of the antiureolytic effect the substances were completely solubilized in a hydroalcoholic solution. Thus, in all studies, substances **3B4** and **3B4a** were bioavailable. However, the substance **3B4a** interacts with the colloids present in the soil, as it is protonated at the soil pH, which reduces its bioavailability and activity.

To evaluate the **3B4**- and **3B4a**-urease supramolecular complexes' stabilities at the urease catalytic site, MD simulations were performed using the docking poses as initial conformation. For both derivatives, the system acquires stability after 20 ns of simulation and remains until the end of the simulations. The RMSD values (Figure 5a) from their docking poses showed minimal deviations (between 0.1 and 0.3 nm), indicating that the molecular docking results are reliable. In addition, the RMSF plots (Figure 5b) show low fluctuations (between 0.1 and 0.5 nm), with emphasis on smaller changes for the residues that coordinate with nickel (His^{407}, His^{409}, KCX^{490}, His^{492}, His^{519}, and His^{545}). Finally, MM-PBSA calculations were applied to determine the binding energy of the complexes with the urease. The results showed that the binding energy value for derivative **3B4a** (ΔG_{bind} = –46.65 ± 0.43 kJ mol^{-1}) is about two times lower than the binding energy value for **3B4** (ΔG_{bind} = –20.38 ± 0.83 kJ mol^{-1}), which agrees with binding constants (K_b) which were experimentally calculated for both compounds.

Binding and thermodynamic parameters of macromolecule-ligand

Figure 6 illustrates the spectral emission profile of urease (1 μM) at different concentrations of **3B4** and **3B4a** (5-80 μM) at pH 7.4 and 30 °C (the spectral profiles for the other temperatures evaluated can be accessed in

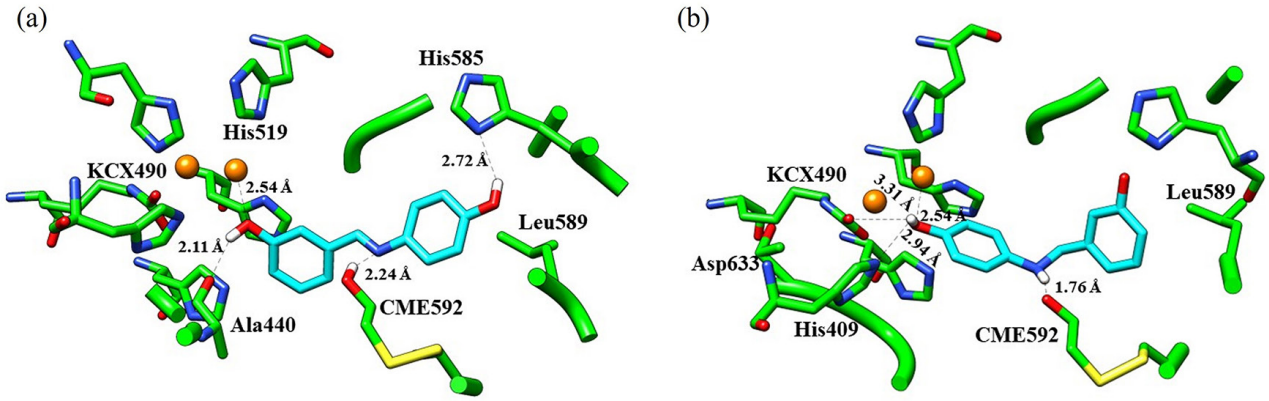

Figure 4. Interactions of **3B4** (a) and **3B4a** (b) with Ni metals and residues from urease. The binding conformation of the ligands is shown in stick representation, and orange spheres represent the two Ni^{II} ions. Coordination with Ni^{II} and hydrogen bonding are dotted lines.

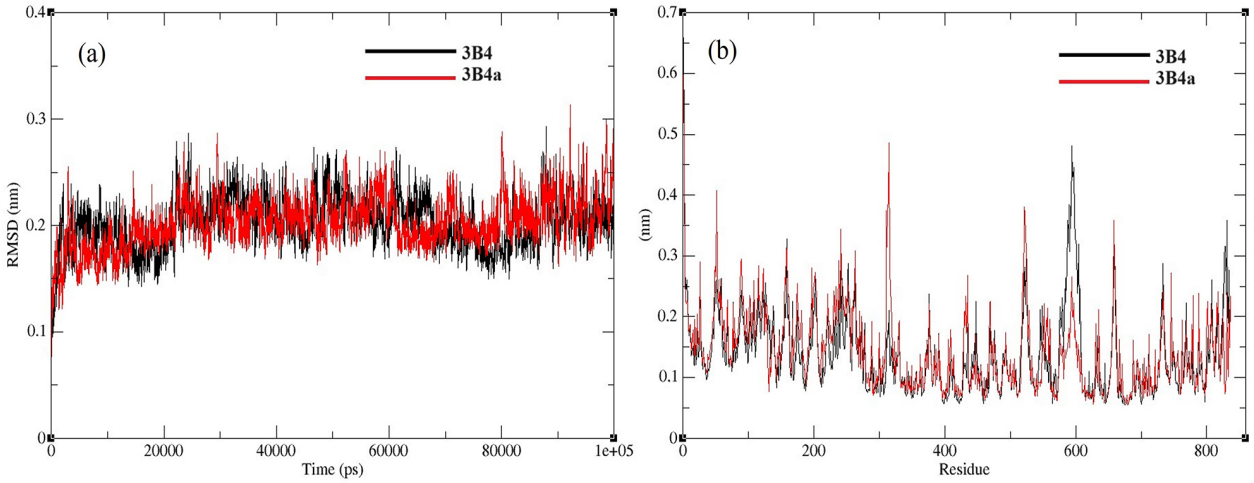

Figure 5. RMSD plots for the ligands (a) and RMSF plots for the backbone Cα atoms of the urease (b) with sequential numbering from the PDB.

Figure S7, SI section). In Figure 6 it is also possible to observe the Stern-Volmer quenching plot and double logarithmic curves for calculating the binding constant of substances (**3B4** and **3B4a**). As can be seen, urease showed an intense fluorescence band between 334 nm when excited at 280 nm (Figures 6a and 6d). It is also possible to observe that increasing concentrations of the inhibitors (**3B4** and **3B4a**) led to a reduction in the fluorescence intensity (quenching process) associated with a bathochromic displacement (Figures 6a and 6d). This spectral profile may be related to conformational alterations of the enzyme, resulting from the interaction with inhibitors, and changes in the microenvironment of Trp and Tyr residues, causing an increase in polarity (water presence) around these residues,[46] and will be covered in the 3D fluorescence study. Different interactions at the molecular level can result in quenching, such as excited-state reactions, molecular rearrangement, transfer of energy, ground-state complex formation, and collisional quenching. Consequently, changes or perturbations in fluorescence properties like quantum yield, intensity, and/or lifetime are observed.[47]

It is possible to determine the quenching process by evaluating the constant k_q, whose values are illustrated in Table 1. When k_q is less than 2.0×10^{10} M^{-1} s^{-1}, quenching tends to be predominantly dynamic, while higher values of k_q indicate that quenching will be mostly static.[48] From these results, it is possible to infer that the suppression of the intrinsic fluorescence of the enzyme by the two inhibitors (**3B4** and **3B4a**) occurs through static quenching. Static quenching occurs in the ground state, resulting in the formation of a non-fluorescence-emitting complex between the fluorophore and the quenching agent.[47] The k_q range for substance **3B4** was between 0.51 and 0.85 × 10^{12} M^{-1} s^{-1} and for substance **3B4a** from 0.84 to 1.16 × 10^{12} M^{-1} s^{-1}, exceeding the limiting diffusional constant, showing the predominance of static quenching.

The degree of interaction between the compounds was evaluated using the K_b (binding constant), and the stoichiometry of the complex urease:inhibitors (*n*) were determined (Table 1). The increase in K_b and temperature between the enzyme and **3B4** or **3B4a** suggests that the rise in temperature favors the formation of the complex. The **3B4**-urease complex presented a stoichiometry that varied between 0.73 to 0.95; while the **3B4a**-urease complex varied from 1.53 to 1.63 in relation to increasing temperature. In general, **3B4a** showed higher K_b values (9.55-41.69 × 10^5 M^{-1}) than **3B4** (0.004-0.04 × 10^5 M^{-1}), suggesting a stronger interaction with the enzyme. This result agrees with the molecular modeling study, where a more stable **3B4a**-urease complex was observed. Literature data also point out to interaction involving urease and other organic compounds, such as K_b around 6.6-84.9 × 10^5 M^{-1} for Biginelli adducts,[45] around 5.71-7.95 × 10^3 M^{-1} for *N*-carbamothioylbenzamide,[41] and

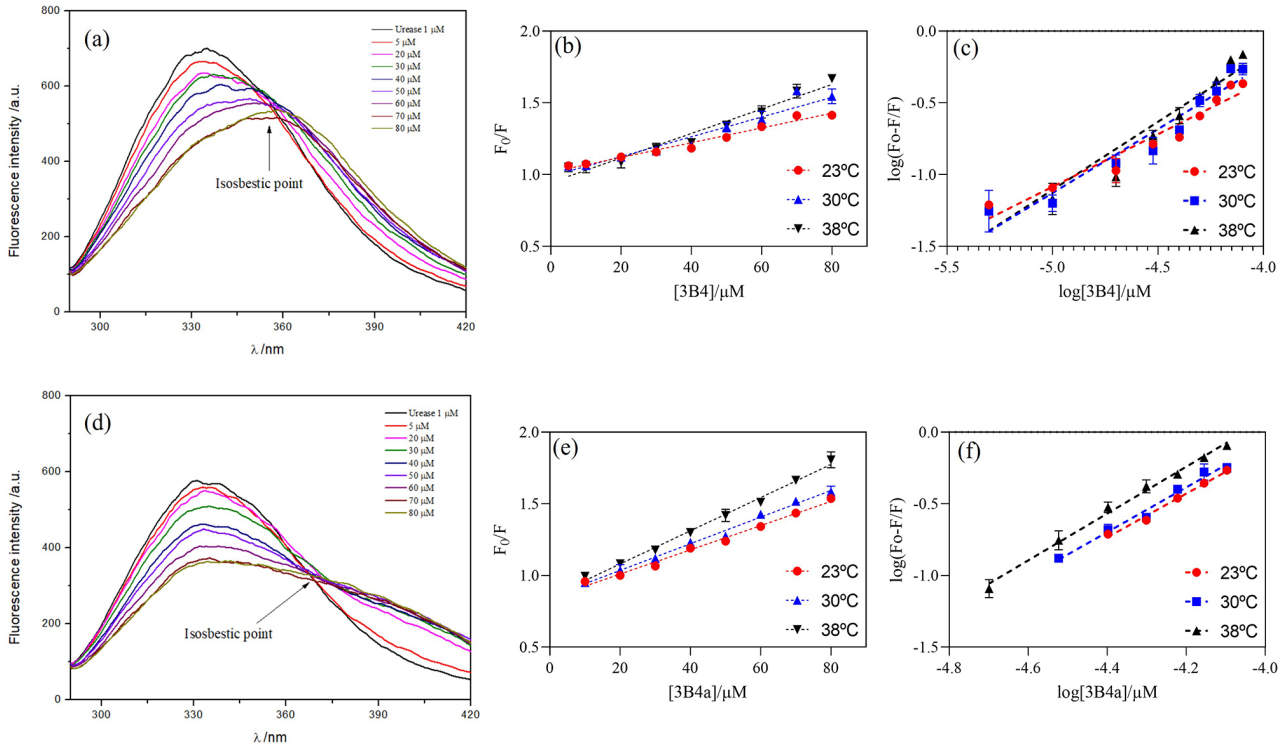

Figure 6. Emission spectral profile of urease (1 μM) at different concentrations of **3B4** (a) and **3B4a** (d) (5-80 μM) at pH 7.4 and 30 °C; Stern-Volmer quenching plot for **3B4** (b) and **3B4a** (e) at 23, 30 and 38 ºC; double logarithmic curve to binding constant calculation for **3B4** (c) and **3B4a** (f) at 23, 30, 38 ºC.

Table 1. Binding and thermodynamics parameters of urease interaction with **3B4** and **3B4a** at different temperatures (23, 30, and 38 °C)

Substance	T / (°C)	Stern-Volmer constant			Binding parameters			Thermodynamic parameters			
		K_{SV} / (10^3 M^{-1})	r	k_q / (10^{12} M^{-1} s^{-1})	K_b / (10^5 M^{-1})	*n*	r	ΔG / (kJ mol^{-1})	ΔH / (kJ mol^{-1})	ΔS / (J mol^{-1} K^{-1})	Preferred interactions
3B4	23	5.14 ± 0.18	0.9736	0.514	0.0040 ± 0.0001	0.73 ± 0.04	0.9326	–15.179	+116.7	+445.6	hydrophobic forces
	30	6.87 ± 0.37	0.9420	0.687	0.020 ± 0.001	0.89 ± 0.06	0.9126	–18.298			
	38	8.53 ± 0.39	0.9500	0.853	0.040 ± 0.001	0.95 ± 0.06	0.9116	–21.863			
3B4a	23	8.45 ± 0.20	0.9885	0.845	9.55 ± 0.39	1.53 ± 0.04	0.9892	–33.650	+75.8	+369.7	hydrophobic forces
	30	9.29 ± 0.26	0.9830	0.929	14.83 ± 0.77	1.56 ± 0.09	0.9569	–36.238			
	38	11.58 ± 0.30	0.9849	1.158	41.69 ± 1.14	1.63 ± 0.05	0.9820	–39.195			

3B4: 4-(3-hydroxybenzylideneamino) phenol; **3B4a**: 3-(((4-hydroxyphenyl)amino)methyl)phenol; T: temperature; K_{SV}: Stern-Volmer constant; K_b: binding constant; *n*: binding site number; r: linear correlation coefficient; k_q: maximum rate constant for diffusional quenching bimolecular constant in biopolymer systems; ΔG: Gibbs free energy; ΔH: enthalpy variation; ΔS: entropy variation.

around 18.6-52.5 × 10^5 M^{-1} for (+)-usnic acid.[46] Thus, the substance **3B4a** appears more similar to Biginelli adducts and (+)-usnic acid, while substance **3B4** is more similar to *N*-carbamothioylbenzamide.

The thermodynamic parameters of **3B4** and **3B4a** (Table 1) were calculated using equation 3, described in the Experimental section. Figure S8 (SI section) shows a graphical representation of the linearized Van't Hoff equation for **3B4** and **3B4a**. From these parameters, it was possible to determine the predominant types of intermolecular bonds in the interaction process. When $\Delta H > 0$ and $\Delta S > 0$, hydrophobic forces are predominant; for $\Delta H < 0$ and $\Delta S < 0$, there is a predominance of van der Waals forces and hydrogen bonds; and when $\Delta H < 0$ and $\Delta S > 0$, there is a predominance of electrostatic interactions.[46] Thus, there is evidence that hydrophobic interactions are the preferential forces in the formation of the urease-**3B4** and urease-**3B4a** complexes, which could be expected given the high hydrophobicity of these substances, observed in solubility studies (Table S1, SI section). The interaction process is entropically favorable, and the negative values observed for ΔG indicate that the interaction between urease and **3B4** or **3B4a** is thermodynamically favored. Additionally, the ΔG values obtained in fluorescence studies are in agreement with the ΔG_{bind} obtained in theoretical molecular docking studies, showing higher values for **3B4a** than for substance **3B4**.

Substances **3B4** and **3B4a** have functional groups that favor hydrogen bonds with the active site of the urease enzyme, as demonstrated in the molecular docking study. However, the presence of aromatic groups results in preferential interactions of hydrophobic forces, observed in the calculated thermodynamic parameters. A qualitative study to evaluate the solubility of **3B4** and **3B4a** showed that both substances are insoluble in water and aqueous solutions (Table S1, SI section). Furthermore, calculations performed on the Chemicalize[40] platform indicated a logP of 3.24 for **3B4** and 2.56 for **3B4a** (Figure S9, SI section), providing further evidence of the lipophilicity of these substances.

Nonpolar molecules tend to self-associate in aqueous solution. The association of two nonpolar molecules in water decreases the nonpolar surface area, which reduces the amount of structured water and thus generates a favorable entropy of association. The enthalpy contribution to hydrophobic interactions is due to the presence of water molecules that occupy hydrophobic binding sites, interfering with the formation of hydrogen bonds with the receptor.[49] Thus, it is suggested that hydrophobic forces are also relevant in substance-enzyme and substance-solvent interactions.

Evaluation of conformational changes in the urease: 3D fluorescence studies

3D fluorescence studies were performed to investigate the bathochromic displacement observed from the addition of increasing concentrations of **3B4** or **3B4a**, which may be evidence of possible alterations in the urease's secondary structure and the fluorophore residue's microenvironment. Figures 7 and S10 (SI section) illustrate the 3D fluorescence spectra for free urease and the complexes with **3B4** (Figure 7b) or **3B4a** (Figure S10b). These spectra have three emission peaks: (*i*) scattering Rayleigh that occurs at $\lambda_{ex} = \lambda_{em}$; (*ii*) fluorescence from the amino acid residues Trp and Tyr; and (*iii*) fluorescence from the highly excited electronic states of the aromatic residues composing the protein structure.[41] As can be seen, there is a significant decrease in the fluorescence of peaks 2 and 3. The main parameters obtained for 3D fluorescence spectra and the Stokes displacement are summarized in Table 2, with the position and fluorescence intensity of the maximum emission peaks.

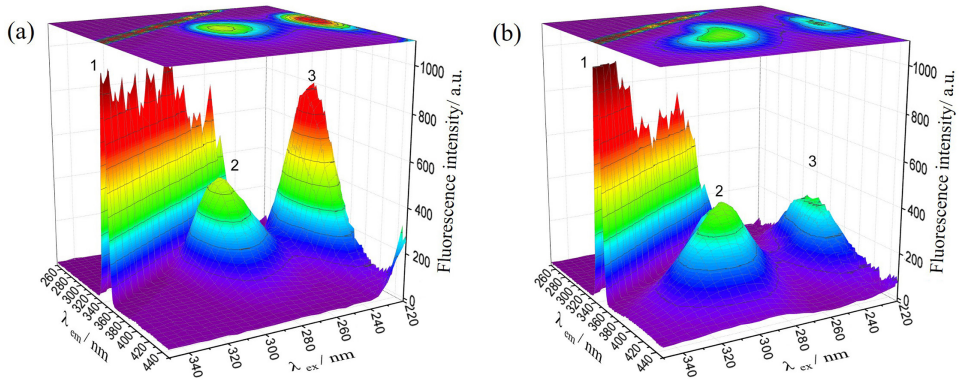

Figure 7. 3D fluorescence analysis of the effect of urease (1 μM) before (a) and after adding **3B4** (b) (70 μM) at pH 7.4.

Table 2. 3D fluorescence parameters for the free urease and complex urease-**3B4** or urease-**3B4a**. Conditions: urease at 1.0 μM, **3B4** or **3B4a** 70 μM, and pH 7.40

Peak	Free urease (urease)			Urease + **3B4**		
	Position ($\lambda_{ex}/\lambda_{em}$)	Stokes shift / nm	I_F	Position ($\lambda_{ex}/\lambda_{em}$)	Stokes shift / nm	I_F
1	$\lambda_{ex} = \lambda_{em}$	0	943	$\lambda_{ex} = \lambda_{em}$	0	100
2	280 / 338	58	438 (100%)	285 / 364	79	343 (78%)
3	225 / 335	110	817 (100%)	230 / 348	118	381 (38%)
Peak	Free urease (Urease)			Urease + **3B4a**		
	Position ($\lambda_{ex}/\lambda_{em}$)	Stokes shift / nm	I_F	Position ($\lambda_{ex}/\lambda_{em}$)	Stokes shift / nm	I_F
1	$\lambda_{ex} = \lambda_{em}$	0	810	$\lambda_{ex} = \lambda_{em}$	0	100
2	282/334	52	528 (100%)	287/333	46	343 (65%)
3	234/334	110	873 (100%)	229/337	108	381 (44%)

Stokes shift: relative to Stokes displacement, where $\Delta\lambda = \lambda_{em} - \lambda_{ex}$. I_F: fluorescence intensity. **3B4**: 4-(3-hydroxybenzylideneamino) phenol; **3B4a**: 3-(((4-hydroxyphenyl)amino)methyl)phenol.

From the results presented above, it was possible to observe that **3B4** and **3B4a** led to similar spectral profiles (Figures 7 and S10), with a reduction of fluorescence intensity of peaks 2 and 3 by 78 and 38%, respectively, in the presence of **3B4** and by 65 and 44% for **3B4a**, indicating conformational changes in the region of Tyr and Trp residues of urease enzyme. The decrease in emission at peak 3 could be linked to alterations in molecular structure that reduce the visibility of aromatic amino acid residues. This alteration makes energy absorption more intricate, subsequently reducing transitions to excited states that typically cause strong fluorescence emission, resembling the behavior observed in the free enzyme.[41] Stokes displacement (peak 2), observed for longer wavelengths in the presence of **3B4** and for shorter wavelengths for **3B4a**, represents conformational changes in the native protein structure, making the microenvironment of interaction more polar and apolar, respectively.

Competition assay

The inhibition mechanism of the **3B4** and **3B4a** was evaluated in the presence of urea (urease enzyme substrate) and classical/commercial inhibitors (HU and NBPT). The ratio between binding constants in the presence and absence of competitors and substrate (K_b'/K_b) was used to assess the influence on urease-**3B4** and urease-**3B4a** interactions. K_b' and K_b are the binding constants in the presence and absence of a competitor/substrate, respectively. The formation of the urease-inhibitor complex is favored in the presence of the competitor/substrate when $K_b'/K_b > 1$; and disadvantaged when $K_b'/K_b < 1$ (Table 3).

Analyzing the ratios between K_b' and K_b, it can be observed that the binding constant decreased notably in the presence of the enzyme-substrate (urea). Therefore, complex formation decreased in the presence of urea, which strongly indicates that **3B4** and **3B4a** interact in the active site of the enzymes, competing with urea for it. NBPT is a mixed-type commercial inhibitor.[50] Thus, the ligand can bind to the enzyme's active site or other regions, modifying its conformation and inhibiting the enzymatic activity. HU is a competitive type inhibitor, interacting directly at the enzyme's active site.[51] In the presence of these competitors, the formation of the urease-**3B4** or **3B4a** complex is

Table 3. Relationship of urease binding constants in the absence (K_b) and presence (K_b') of the substrate (urea) or classical urease inhibitors. Conditions: 1.0 μM urease, 10 μM substrate or inhibitor, **3B4** and **3B4a** (5-80 μM)

Substance	Substrate	Binding constant ratio (K_b'/K_b)[a]	
		Competitive inhibitors	
	Urea	HU	NBPT
3B4	0.03	2.24	9.41
3B4a	0.02	8.99	41.88

[a]K_b'/K_b: ratio between the binding constants in the presence and absence of competitors and substrate. **3B4**: 4-(3-hydroxybenzylideneamino) phenol; **3B4a**: 3-(((4-hydroxyphenyl)amino)methyl)phenol; HU: hydroxyurea; NBPT: *N*-(butyl) thiophosphoric triamide.

favored, which suggests that both substances do not interact only in the active site of the enzyme. However, in NBPT presence, the constants ratio (K_b'/K_b) is much larger for **3B4a** than for **3B4**. As NBPT is a mixed inhibitor, there is less competition, which might suggest that the preferred binding site for **3B4a** might be the active site. There is also the possibility that the interaction of NBPT with other parts of the enzyme is causing a change in the conformation of the active site, favoring the binding with **3B4** and **3B4a**, or these ligands, in particular **3B4a**, are interacting with the active site of the enzyme, as well as with a different allosteric site other than NBPT.

Interaction between urea and **3B4** or **3B4a**

FTIR is a technique commonly used to verify interactions between actives and excipients, where the reduction in the intensity or suppression of a peak and the appearance of new peaks are evidence of an interaction.[52] Figure 8a illustrates the spectra obtained for urea (U), **3B4** (I-1) and the urea + **3B4** (1:1) mixture at times 0 (UI1-0 h),

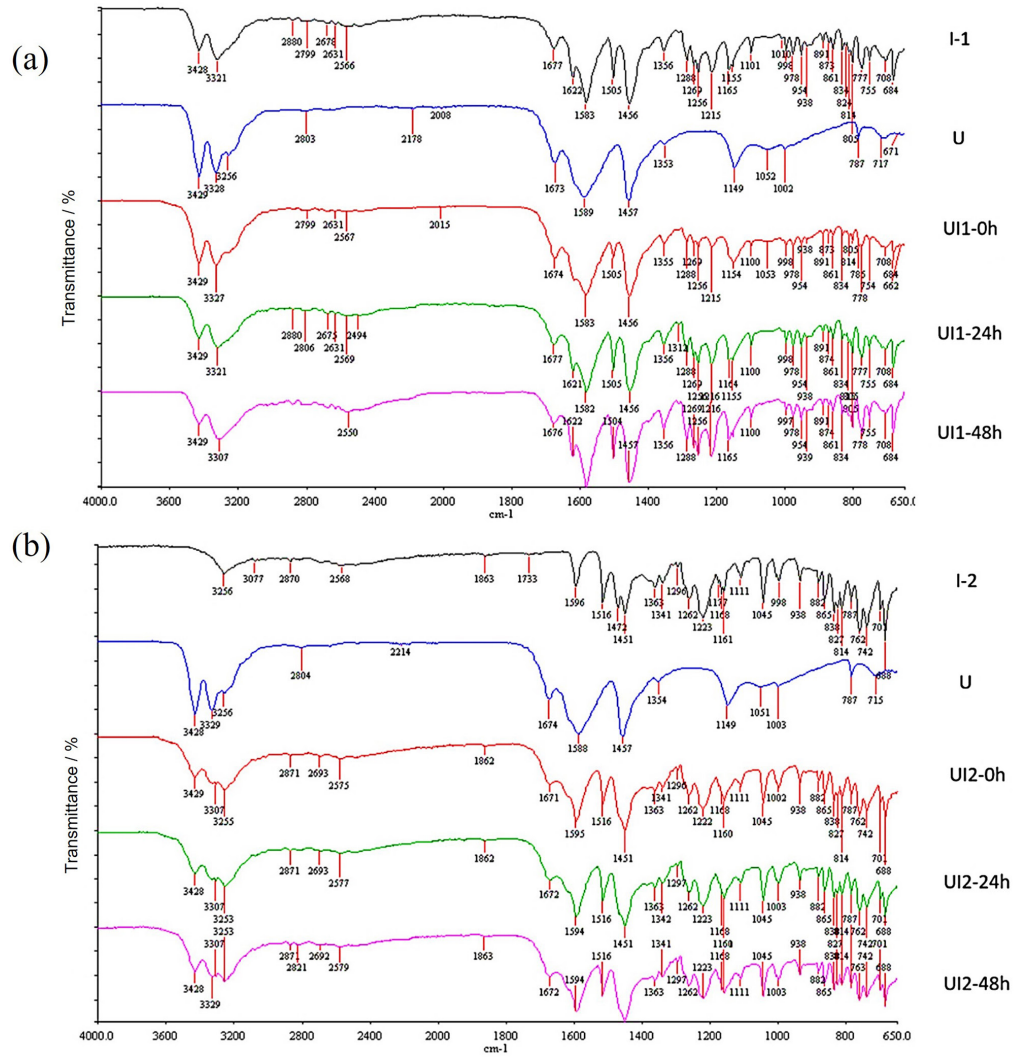

Figure 8. (a) Spectra obtained for urea (U), **3B4** (I-1), and the mixture urea:**3B4** (1:1) at 0 h (UI1-0 h), 24 h (UI1-24 h) and 48 h (UI1-48 h) after preparation of the solutions. (b) Spectra obtained for urea (U), **3B4a** (I-2), and the mixture urea:**3B4a** (1:1) at 0 h (UI2-0h), 24 h (UI2-24h) and 48 h (UI2-48 h) after preparation of the systems.

24 (UI1-24 h) and 48 h (UI1-48 h). Figure 8b illustrates the corresponding spectra for **3B4a**. For urea, there is a characteristic stretching band of the N–H bond at 3428-3429 and 3328-3329 cm^{-1}, a bending band of this bond at 1588-1589 cm^{-1}, and stretching bands for the C=O and C–N bond at 1673-1674 and 1457 cm^{-1}, respectively. The spectrum obtained for **3B4** (Figure 8a) shows a characteristic stretching band of the O–H bond at 3321 cm^{-1} and stretching bands from the C=N and C=C bonds at 1622, 1583, 1505, and 1456 cm^{-1}. For 3B4a (Figure 8b), there is a typical stretching band of the N–H bond at 3256 cm^{-1}, a bending band of the N–H aromatic secondary amine bond at 1516 cm^{-1}, and stretching bands from C=C bonds at 1472-1451 cm^{-1}. The N–H stretching band probably covers the stretching band for the O–H bond.

No significative changes in the spectrum profile were recorded when equal amounts of **3B4** or **3B4a** were added to urea, regardless of the incubation time of the systems at room temperature. However, some bands were masked by others of greater intensity, such as the stretching of the O–H bond in the imine **3B4** and the stretching bands from the C=C bond in the amine **3B4a**. Thus, no interaction between urea and **3B4** or **3B4a** was observed in the experimental conditions tested, which may be evidence of these substances' compatibility for future agriculture applications.

Conclusions

Investment in the development of new urease inhibitors is a worldwide demand. In this work, we evaluated the anti-urease activity of substances **3B4** and **3B4a**, showing that both are promising inhibitors. The results obtained in the molecular modeling showed that the functional groups 3-OH in **3B4** and 4-OH in **3B4a** are essential for the inhibition of the enzyme urease; and that **3B4a** forms a more stable supramolecular complex with the enzyme due to the formation of a hydrogen bond with the amine group. The molecular fluorescence study also proved that the enzyme's interaction with **3B4a** is stronger. Hydrophobic forces are also preferably formed in the inhibitor-urease complex studied and both inhibitors are preferably competitive. Finally, FTIR analyses did not show interactions with urea, providing evidence of compatibility, which is essential for developing a new product for agronomic use. Finally, as perspectives, we propose to evaluate the efficiency and safety of these inhibitors in field studies.

Supplementary Information

The NMR and IR (infrared) spectra obtained in the substance characterization stage; the spectral profile of urease emission at different temperature and concentrations of **3B4** and **3B4a**; the graphical representation of the linearized Van't Hoff equation; the solubility and lipophilicity parameters for **3B4** and **3B4a** are available free of charge at http://jbcs.sbq.org.br as a PDF file.

Acknowledgments

The authors are thankful to the Universidade Federal de Minas Gerais (UFMG) and Universidade Federal de Alagoas (UFAL) for the infrastructure. This work was made possible by the Network for the Development of Novel Urease Inhibitors (REDNIU), which is financially supported by the Coordenação de Aperfeiçoamento de Pessoal de Nível Superior - Brazil (CAPES, Finance Code 001), Conselho Nacional de Desenvolvimento Científico e Tecnológico (CNPq, grants No. 408590/2021-1 and No. 408807/2021-0), Fundação de Amparo à Pesquisa do Estado de Minas Gerais (FAPEMIG, grants No. APQ-03069-18, APQ-02103-23 and RED-00082-23), and Fundação de Amparo à Pesquisa do Estado de Alagoas (FAPEAL, grant No. 60030.0000002362/2022). LVM, JCCS, and AF are recipients of research fellowships from CNPq.

Author Contributions

Caroline S. Dohanik was responsible for methodology, formal analysis, visualization, writing original draft, review and editing; Camila P. Pereira for the methodology, formal analysis, validation, visualization; Breno G. F. Oliveira for the methodology, formal analysis, visualization, review and editing; Amanda L. A. Nascimento for the methodology, formal analysis, validation, visualization; Josué C. C. Santos for the conceptualization, resources, software, methodology, validation, visualization; Igor J. S. Nascimento for the methodology, formal analysis, validation, visualization; Thiago M. de Aquino for conceptualization, resources, software, methodology, validation, writing original draft and visualization; Rachel O. Castilho for the conceptualization, methodology, formal analysis, visualization and supervision; Luzia V. Modolo for the conceptualization, methodology, resources, formal analysis, visualization and supervision; Gisele A. C. Goulart for the conceptualization, resources, methodology, formal analysis, writing original draft, review and editing, visualization and supervision; Ângelo de Fátima for the conceptualization, resources, methodology, writing original draft, review and editing, visualization and supervision.

References

1. Erisman, J. W.; Sutton, M. A.; Galloway, J.; Klimont, Z.; Winiwarter, W.; *Nat. Geosci.* **2008**, *1*, 636. [Crossref]

2. Smil, V.; *Enriching the Earth: Fritz Haber, Carl Bosch, and the Transformation of World Food Production*; MIT press: Cambridge, Massachusetts, USA, 2004.
3. Stewart, W. M.; Dibb, D. W.; Johnston, A. E.; Smyth, T. J.; *Agron. J.* **2005**, *97*, 1. [Crossref]
4. Driver, J. G.; Owen, R. E.; Makanyire, T.; Lake, J. A.; McGregor, J.; Styring, P.; *Front. Energy Res.* **2019**, *7*, 88. [Crossref]
5. Cantarella, H.; Otto, R.; Soares, J. R.; Silva, A. G. B.; *J. Adv. Res.* **2018**, *13*, 19. [Crossref]
6. Krajewska, B.; *J. Mol. Catal. B: Enzym.* **2009**, *59*, 9. [Crossref]
7. Frazão, J. J.; da Silva, Á. R.; da Silva, V. L.; Oliveira, V. A.; Corrêa, R. S.; *Rev. Bras. Eng. Agrícola Ambient.* **2014**, *18*, 1262. [Crossref]
8. Watson, C. J.; Akhonzada, N. A.; Hamilton, J. T. G.; Matthews, D. I.; *Soil Use Manage.* **2008**, *24*, 246. [Crossref]
9. Zaman, M.; Nguyen, M. L.; Šimek, M.; Nawaz, S.; Khan, M. J.; Babar, M. N.; Zam, S. In *Greenhouse Gases - Emission, Measurement and Management*; Guoxiang, L., ed.; InTech, 2012. [Crossref]
10. Sumner, J. B.; *Nobel Lecture*, *The Chemical Nature of Enzymes*, https://www.nobelprize.org/prizes/chemistry/1946/sumner/lecture/, accessed in December 2023.
11. Sumner, J. B.; *J. Biol. Chem.* **1926**, *70*, 97. [Crossref]
12. Dixon, N. E.; Gazzola, C.; Blakeley, R. L.; Zerner, B.; *J. Am. Chem. Soc.* **1975**, *97*, 4131. [Crossref]
13. Mobley, H. L. T.; Island, M. D.; Hausinger, R. P.; *Microbiol. Rev.* **1995**, *59*, 451. [Crossref]
14. Carter, E. L.; Flugga, N.; Boer, J. L.; Mulrooney, S. B.; Hausinger, R. P.; *Metallomics* **2009**, *1*, 207. [Crossref]
15. Camargo, J. A.; Alonso, Á.; *Environ. Int.* **2006**, *32*, 831. [Crossref]
16. Erisman, J. W.; Bleeker, A.; Galloway, J.; Sutton, M. S.; *Environ. Pollut.* **2007**, *150*, 140. [Crossref]
17. Maskell, L. C.; Smart, S. M.; Bullock, J. M.; Thompson, K.; Stevens, C. J.; *Global Change Biol.* **2010**, *16*, 671. [Crossref]
18. Schuurkes, J. A. A. R.; Mosello, R.; *Swiss J. Hydrol.* **1988**, *50*, 71. [Crossref]
19. van Breemen, N.; Burrough, P. A.; Velthorst, E. J.; van Dobben, H. F.; de Wit, T.; Ridder, T. B.; Reijnders, H. F. R.; *Nature* **1982**, *299*, 548. [Crossref]
20. Martikainen, P. J.; *Appl. Environ. Microbiol.* **1985**, *50*, 1519. [Crossref]
21. Martins, M. R.; Sant'Anna, S. A. C.; Zaman, M.; Santos, R. C.; Monteiro, R. C.; Alves, B. J. R.; Jantalia, C. P.; Boddey, R. M.; Urquiaga, S.; *Agric., Ecosyst. Environ.* **2017**, *247*, 54. [Crossref]
22. Barthelmie, R. J.; Pryor, S. C.; *Atmos. Environ.* **1998**, *32*, 345. [Crossref]
23. Wu, Y.; Gu, B.; Erisman, J. W.; Reis, S.; Fang, Y.; Lu, X.; Zhang, X.; *Environ. Pollut.* **2016**, *218*, 86. [Crossref]
24. Xing, Y.-F.; Xu, Y.-H.; Shi, M.-H.; Lian, Y.-X.; *J. Thorac. Dis.* **2016**, *8*, E69. [Crossref]
25. Pinto, V. M.; Bruno, I. P.; de Jong Van Lier, Q.; Dourado Neto, D.; Reichardt, K.; *Coffee Sci.* **2017**, *12*, 176. [Link] accessed in December 2023
26. Modolo, L. V.; da-Silva, C. J.; Brandão, D. S.; Chaves, I. S.; *J. Adv. Res.* **2018**, *13*, 29. [Crossref]
27. Li, Q.; Cui, X.; Liu, X.; Roelcke, M.; Pasda, G.; Zerulla, W.; Wissemeier, A. H.; Chen, X.; Goulding, K.; Zhang, F.; *Sci. Rep.* **2017**, *7*, 43853. [Crossref]
28. Krol, D. J.; Forrestal, P. J.; Wall, D.; Lanigan, G. J.; Sanz-Gomez, J.; Richards, K. G.; *Sci. Total Environ.* **2020**, *725*, 138329. [Crossref]
29. Trenkel, M. E.; *Slow-and Controlled-Release and Stabilized Fertilizers: An Option for Enhancing Nutrient use Efficiency in Agriculture*, 2nd ed; International Fertilizer Association: Paris, France, 2010. [Link] accessed in December 2023
30. Abalos, D.; Sanz-Cobena, A.; Misselbrook, T.; Vallejo, A.; *Chemosphere* **2012**, *89*, 310. [Crossref]
31. Sha, Z.; Lv, T.; Staal, M.; Ma, X.; Wen, Z.; Li, Q.; Pasda, G.; Misselbrook, T.; Liu, X.; *J. Soils Sediments* **2020**, *20*, 2130. [Crossref]
32. Engel, R. E.; Towey, B. D.; Gravens, E.; *Soil Sci. Soc. Am. J.* **2015**, *79*, 1674. [Crossref]
33. Modolo, L. V.; de Fátima, A.; de Souza, L. T.; Horta, L. P.; da Silva, C. M.; Barbosa, G. M.; Ferreira, L. B.; Marriel, I. E.; *WO/2016/174648*, **2016**.
34. Chaves-Silva, S.; Horta, L. P.; Souza, L. T.; da Silva, C. M.; Dohanik, C. S.; Goulart, G. A. C.; Marriel, I. E.; de Fátima, Â.; Modolo, L. V.; *Ind. Crops Prod.* **2019**, *145*, 111995. [Crossref]
35. Byung, T. C.; Sang, K. K.; *Tetrahedron* **2005**, *61*, 5725. [Crossref]
36. da Silva, C. M.: *Síntese de Aldiminas e Calix[4]aldiminas Mediada por Radiação de Micro-ondas e Avaliação de Atividades Antifúngica e Citotóxica*; PhD Thesis, Federal University of Minas Gerais, Belo Horizonte, Brazil, 2013. [Link] accessed in December 2023
37. Huneck, S.; Schreiber, K.; Grimmecke, H. D.; *J. Plant Growth Regul.* **1984**, *3*, 75. [Crossref]
38. Kandeler, E.; Gerber, H.; *Biol. Fertil. Soils* **1988**, *6*, 68. [Crossref]
39. Brito, T. O.; Souza, A. X.; Mota, Y. C. C.; Morais, V. S. S.; de Souza, L. T.; de Fátima, Â.; Macedo, F.; Modolo, L. V.; *RSC Adv.* **2015**, *5*, 44507. [Crossref]
40. *Chemicalize*; ChemAxon Ltd., Budapest, 2018. [Link] accessed in December 2023
41. Tavares, M. C.; Nascimento, I. J. S.; de Aquino, T. M.; Brito, T. O.; Macedo, F.; Modolo, L. V.; de Fátima, Â.; Santos, J. C. C.; *Biophys. Chem.* **2023**, *299*, 107042. [Crossref]
42. Real-Guerra, R.; Carlini, C. R.; Stanisçuaski, F.; *Toxicon* **2013**, *71*, 76. [Crossref]
43. Motulsky, H.; *GraphPad Prism*, version 6.01; GraphPad

Software, Inc., Boston, Massachusetts, USA, 2012. [Link] accessed in December 2023

44. Lopes, A. S.; *Manual Internacional de Fertilidade do Solo*, 2nd ed.; Associação Brasileira para Pesquisa da Potassa e do Fosfato: Piracicaba, Brazil, 1998.
45. Braga, T. C.; Silva, T. F.; MacIel, T. M. S.; da Silva, E. C. D.; da Silva-Júnior, E. F.; Modolo, L. V.; Figueiredo, I. M.; Santos, J. C. C.; de Aquino, T. M.; de Fátima, Â.; *New J. Chem.* **2019**, *43*, 15187. [Crossref]
46. Lage, T. C. A.; Maciel, T. M. S.; Mota, Y. C. C.; Sisto, F.; Sabino, J. R.; Santos, J. C. C.; Figueiredo, I. M.; Masia, C.; de Fátima, Â.; Fernandes, S. A.; Modolo, L. V.; *New J. Chem.* **2018**, *42*, 5356. [Crossref]
47. Lichota, A.; Szabelski, M.; Krokosz, A.; *Int. J. Mol. Sci.* **2022**, *23*, 12382. [Crossref]
48. de Barros, W. A.; Nunes, C. S.; Souza, J. A. C. R.; Nascimento, I. J. S.; Figueiredo, I. M.; de Aquino, T. M.; Vieira, L.; Farias, D.; Santos, J. C. C.; de Fátima, Â.; *Curr. Res. Toxicol.* **2021**, *2*, 386. [Crossref]
49. Schaeffer, L. In *The Practice of Medicinal Chemistry*, 3rd ed.; Wermuth, C. G., ed.; Elsevier/Academic Press: Cambridge, Massachusetts, USA, 2008.
50. Upadhyay, L. S. B.; *Indian J. Biotechnol.* **2012**, *11*, 381. [Crossref]
51. Nelson, D. L.; Cox, M. M.; *Princípios da Bioquímica de Lehninger*, 6th ed.; Artmed Editora: Porto Alegre, Brazil, 2014.
52. Liltorp, K.; Larsen, T. G.; Willumsen, B.; Holm, R.; *J. Pharm. Biomed. Anal.* **2011**, *55*, 424. [Crossref]

Submitted: October 13, 2023
Published online: January 10, 2024